# On the Effect of Mutual Coupling in One-Bit Spatial Sigma-Delta Massive MIMO Systems

Hessam Pirzadeh\*, Gonzalo Seco-Granados<sup>†</sup>, A. Lee Swindlehurst\*, and Josef A. Nossek<sup>§</sup>
\*Center for Pervasive Commun. & Computing, UC Irvine, USA. Email: {hpirzade, swindle}@uci.edu

†Dept. of Telecom. & Systems Eng., Univ. Autònoma de Barcelona, Spain. Email: gonzalo.seco@uab.cat

§Dept. of Teleinformatics Eng., Federal Univ. of Ceara, Brazil. Email: josef.a.nossek@tum.de

Abstract—The one-bit spatial Sigma-Delta concept has recently been proposed as an approach for achieving low distortion and low power consumption for massive multi-input multi-output systems. The approach exploits users located in known angular sectors or spatial oversampling to shape the quantization noise away from desired directions of arrival. While reducing the antenna spacing alleviates the adverse impact of quantization noise, it can potentially deteriorate the performance of the massive array due to excessive mutual coupling. In this paper, we analyze the impact of mutual coupling on the uplink spectral efficiency of a spatial one-bit Sigma-Delta massive MIMO architecture, and compare the resulting performance degradation to standard onebit quantization as well as the ideal case with infinite precision. Our simulations show that the one-bit Sigma-Delta array is particularly advantageous in space-constrained scenarios, can still provide significant gains even in the presence of mutual coupling when the antennas are closely spaced.

#### I. INTRODUCTION

Power consumption is a key concern for next-generation wireless networks. Deploying power efficient base stations (BSs) while satisfying high-data-rate demands is of crucial importance. Massive multiple-input multiple-output (MIMO) architectures are considered to be an important component of next-generation systems to meet the aforementioned objectives, but the high power consumption required by large arrays employing high-resolution analog-to-digital converters (ADCs) poses some practical problems. Hence, the use of low-resolution ADCs with reduced power consumption has gained attention in recent years [1]-[6].

Recently, a spatial Sigma-Delta ( $\Sigma\Delta$ ) architecture has been proposed to compensate for the performance loss due to the use of one-bit quantization in massive MIMO systems [7]-[10]. In this architecture, either the users of interest are assumed to lie within some known angular sector (e.g., as in a sectorized wireless cell), or the array is assumed to be spatially oversampled (antennas spaced less than one-half wavelength  $\lambda$  apart), so that a spatial analog of the classical  $\Sigma\Delta$  approach can be used to shape the quantization noise to angles away from the users' desired directions of arrival (DoAs). Unlike temporal oversampling, there is a limit to the amount of spatial oversampling that can be achieved, due to the physical dimensions of the antennas. In addition, the impact

This work was supported by the U.S. National Science Foundation under Grants CCF-1703635 and ECCS-1824565.

of mutual coupling may become significant as the antenna spacing decreases [11], [12]. While [8] has shown that the low-complexity one-bit  $\Sigma\Delta$  architecture can achieve performance approaching that of systems with high-resolution ADCs, this prior work did not consider the mutual coupling effect.

In this paper, we investigate the impact of mutual coupling on the performance of the spatial  $\Sigma\Delta$  approach assuming a uniform linear array (ULA) of antennas. Our results show that the one-bit Sigma-Delta array is particularly advantageous in space-constrained scenarios, and can still provide significant gains even in the presence of mutual coupling when the antennas are closely spaced. For very small antenna spacings, the noise shaping gain is offset by the loss due to mutual coupling, and the performance remains relatively constant; this is in contrast to a standard high-resolution ADC architecture without  $\Sigma\Delta$ , where the performance degrades monotonically as the antennas move closer together.

*Notation*: We use boldface letters to denote vectors, and capitals to denote matrices. The (i,j)-th element of matrix A and the i-th element of vector a are denoted by  $[A]_{ij}$  and  $a_i$ , respectively. The symbols  $(.)^*$ ,  $(.)^T$ , and  $(.)^H$  represent conjugate, transpose, and conjugate transpose, respectively. A circularly-symmetric complex Gaussian (CSCG) random vector with zero mean and covariance matrix  $R_v$  is denoted by  $v \sim CN(\mathbf{0}, R_v)$ .  $Ci(x) \triangleq \gamma + \log(x) + \int_0^x \frac{\cos(t) - 1}{t} dt$ , and  $Si(x) \triangleq \int_0^x \frac{\sin(t)}{t} dt$  denote cosine and sine integrals where  $\gamma$  is the Euler-Mascheroni constant.  $\mathbb{E}[.]$ ,  $\Re\{.\}$  and  $\Im\{.\}$  represent the expectation operator, the real part and imaginary part of a complex value, respectively. We use diag (x) as the diagonal matrix formed from the elements of vector x.

## II. SYSTEM MODEL

# A. Channel Model and Mutual Coupling

Consider the uplink of a single-cell multi-user MIMO system consisting of K single-antenna users that send their signals simultaneously to a BS equipped with a uniform linear array (ULA) with M antennas. The  $M \times 1$  signal received at the BS from the K users is given by

$$x = GP^{\frac{1}{2}}s + n, \tag{1}$$

where  $G = [g_1, \dots, g_K] \in \mathbb{C}^{M \times K}$  is the channel matrix between the users and the BS, and P is a diagonal matrix whose kth diagonal element,  $p_k$ , represents the transmitted power of

the k-th user. The scalar symbols transmitted by the users are collected in the vector  $\mathbf{s} \in \mathbb{C}^{K \times 1}$ , where  $\mathbb{E}\left\{\mathbf{s}\mathbf{s}^H\right\} = \mathbf{I}_K$  and the symbols are assumed to be independently drawn from a CSCG codebook. The term  $n \sim CN(0, R_n)$  denotes additive CSCG receiver noise at the BS.

For the kth user, the channel vector is modeled as

$$\boldsymbol{g}_k = \sqrt{\frac{\beta_k}{L}} \boldsymbol{T} \boldsymbol{A}_k \boldsymbol{h}_k, \tag{2}$$

where  $\beta_k$  models geometric attenuation and shadow fading, the columns of the  $M \times L$  matrix  $A_k$  are steering vectors corresponding to signal arrivals from different DoAs, and  $h_k$ represents fast-fading channel coefficients that are assumed to be independently and identically distributed as CN(0,1)random variables. The matrix T models the mutual coupling:

$$T = \left(I + \frac{1}{R}Z\right)^{-1} \tag{3}$$

where R denotes the low-noise amplifier (LNA) input impedance. Assuming thin half-wavelength dipoles, the elements of **Z** can be characterized as [13]

$$\begin{split} [\boldsymbol{Z}]_{ij} &= 30 \bigg( 2 \mathrm{Ci}(2\pi d_{ij}) - \mathrm{Ci}(\xi_{ij} + \pi) - \mathrm{Ci}(\xi_{ij} - \pi) \\ &+ j \left( -2 \mathrm{Si}(2\pi d_{ij}) + \mathrm{Si}(\xi_{ij} + \pi) + \mathrm{Si}(\xi_{ij} - \pi) \right) \bigg), \ i \neq j \end{split}$$

$$[\mathbf{Z}]_{ii} = 30(\gamma + \log(2\pi) - \text{Ci}(2\pi) + j\text{Si}(2\pi)),$$
 (4)

where  $d_{ij}$  is the distance between antennas i and j normalized by the wavelength, and  $\xi_{ij} = \pi \sqrt{1 + 4d_{ij}^2}$ .

Since we will be focusing on situations where the signals of interest arrive within a certain angular sector, we assume a physical channel model in which the angular domain for each user is described by L fixed DoAs, as in [15]. Hence,  $A_k$  has columns defined by the steering vectors

$$\boldsymbol{a}\left(\theta_{k\ell}\right) = \left[1, e^{-j2\pi d_{12}\sin(\theta_{k\ell})}, \cdots, e^{-j2\pi d_{1M}\sin(\theta_{k\ell})}\right]^{T}, \quad (5)$$

for DoAs  $\theta_{k\ell}$ . The channels for each user are further distinguished by independent fast fading coefficients, which we collect in the matrix  $\mathbf{H} = [\mathbf{h}_1, \cdots, \mathbf{h}_K] \in \mathbb{C}^{L \times K}$ .

The presence of mutual coupling will not only affect the channel, but will also in general produce colored noise at the receiver. For the mutual coupling model described above, the covariance  $R_n$  of the additive noise can be derived as [14]

$$\begin{split} & \boldsymbol{R_n} = \\ & \boldsymbol{T} \left( \sigma_i^2 \left( \boldsymbol{Z} \boldsymbol{Z}^H + R_N^2 \boldsymbol{I} - 2R_N \Re(\rho^* \boldsymbol{Z}) \right) + 4kTB\Re(\boldsymbol{Z}) \right) \boldsymbol{T}^H, \quad (6 \end{split}$$

#### B. $\Sigma\Delta$ Quantization

In a standard implementation involving one-bit quantization, each antenna element at the BS is connected to a one-bit ADC. In such systems, the received baseband signal at the mth antenna becomes

$$y_m = Q_m(x_m) , (7)$$

where  $Q_{m}\left( .\right)$  denotes the one-bit quantization operation applied separately to the real and imaginary parts as

$$Q_m(x_m) = \alpha_{m,r} \operatorname{sign}(\Re(x_m)) + j\alpha_{m,i} \operatorname{sign}(\Im(x_m)) . \tag{8}$$

The output voltage levels of the one-bit quantizers are represented by  $\alpha_{m,r}$  and  $\alpha_{m,i}$ . While the output level is irrelevant for standard one-bit quantization, for  $\Sigma\Delta$  quantization the selection of adequate output levels is of critical importance, as discussed in [8]. Furthermore, we allow these levels to be a function of the antenna index m, although once the values of  $\alpha_{m,r}$  and  $\alpha_{m,i}$  are chosen, they remain fixed and independent of the user scenario or channel realization. After quantization, the received baseband signal at the BS is given by

$$y = Q(x) = [Q_1(x_1), Q_2(x_2), \cdots, Q_M(x_M)]^T$$
. (9)

By appropriately designing the output voltages of the ADCs (see [8] for details), the received baseband signal at the BS after  $\Sigma\Delta$  quantization becomes

$$\mathbf{y} = \mathbf{x} + \mathbf{U}^{-1} \mathbf{q} \,, \tag{10}$$

in which

$$U = \begin{bmatrix} 1 & & & & & \\ e^{-j\phi} & 1 & & & & \\ \vdots & \ddots & \ddots & & \\ e^{-j(M-1)\phi} & \dots & e^{-j\phi} & 1 \end{bmatrix},$$
(11)

where  $\phi$  denotes the center angle of the sector with low quantization noise, and q represents the effective quantization noise. Following the same reasoning as in [8], the covariance matrix of the quantization noise can be approximated as

$$R_q \simeq \operatorname{diag}\left(p_q\right),$$
 (12)

where

$$\boldsymbol{p_q} = \left(\frac{\pi}{2}\zeta - 1\right)\boldsymbol{\Pi}\boldsymbol{p_x} \tag{13}$$

$$\mathbf{p}_{x} = \left[ \mathbb{E}\left[ |x_{1}|^{2} \right], \mathbb{E}\left[ |x_{2}|^{2} \right], \cdots, \mathbb{E}\left[ |x_{M}|^{2} \right] \right]^{T}$$
 (14)

$$R_{n} = T \left( \sigma_{i}^{2} \left( \mathbf{Z} \mathbf{Z}^{H} + R_{N}^{2} \mathbf{I} - 2R_{N} \Re(\rho^{*} \mathbf{Z}) \right) + 4kTB\Re(\mathbf{Z}) \right) T^{H}, \quad (6)$$

$$\text{with } \mathbb{E} \{ \mathbf{i}_{N} \mathbf{i}_{N}^{H} \} = \sigma_{i}^{2} \mathbf{I}, \quad \mathbb{E} \{ \mathbf{u}_{N} \mathbf{u}_{N}^{H} \} = \sigma_{u}^{2} \mathbf{I}, \quad R_{N} = \frac{\sigma_{u}}{\sigma_{i}},$$

$$\mathbb{E} \{ \mathbf{u}_{N} \mathbf{i}_{N}^{H} \} = \frac{\rho}{\sigma_{u} \sigma_{i}} \mathbf{I}, \quad \text{where } \mathbf{i}_{N} \text{ and } \mathbf{u}_{N} \text{ denote the equivalent noise current and voltage of the low noise amplifier (LNA), and  $k, T, \text{ and } B \text{ represent the Boltzman constant, environment temperature, and bandwidth, respectively.}$ 

$$1 \quad (\frac{\pi}{2} \zeta - 1)^{m} \quad 1 \quad (\frac{\pi}{2} \zeta - 1)^{m} \quad 1 \quad (\frac{\pi}{2} \zeta - 1)^{m} \quad \dots \quad (\frac{\pi}{2} \zeta - 1) \quad 1$$$$

and  $\zeta = 1.13$  is a correction factor. In the following sections, we investigate the spectral efficiency of the system described above and study the impact of antenna spacing.

#### III. SPECTRAL EFFICIENCY

Due to the complicated structure of the mutual coupling matrix in (3) and the quantization noise shaping matrix  $U^{-1}$ , a closed-form expression for the spectral efficiency (SE), if it exists, would likely not provide significant insight into its behavior with respect to antenna spacing, nor would it provide a tool for the purpose of optimization. Hence, in the next section we numerically evaluate the SE of the system.

The received  $\Sigma\Delta$ -quantized signal, v, at the BS is

$$y = Q(x) = GP^{\frac{1}{2}}s + n + U^{-1}q$$
 (15)

The total effective noise  $\eta = n + U^{-1}q$  has covariance matrix  $R_{\eta} = R_n + U^{-1}R_qU^{-H}$ . We assume the BS employs a linear receiver W, and we will consider the case of maximum ratio combining (MRC) and zero-forcing (ZF). For MRC, we do not account for the fact that  $R_n$  is spatially colored, since prewhitening G destroys the approximate orthogonality of the array response and increases the inter-user interference. Thus, for MRC we set W = G. However, knowledge of  $R_{\eta}$  can be exploited by the ZF receiver, and thus we assume the prewhitened solution  $W = R_{\eta}^{-1}G(G^HR_{\eta}^{-1}G)^{-1}$ . For either receiver, the detected symbol vector is

$$\hat{s} = W^{H} y = W^{H} G P^{\frac{1}{2}} s + W^{H} n + W^{H} U^{-1} q.$$
 (16)

The k-th detected symbol can be written as

$$\hat{s}_k = \sqrt{p_k} \mathbf{w}_k^H \mathbf{g}_k s_k + \sqrt{p_k} \mathbf{w}_k^H \sum_{i \neq k} \mathbf{g}_i s_i + \mathbf{w}_k^H \mathbf{n} + \mathbf{w}_k^H \mathbf{U}^{-1} \mathbf{q},$$
(17)

where  $\mathbf{w}_k$  is the kth column of  $\mathbf{W}$ . We assume the BS treats  $\mathbf{w}_k^H \mathbf{g}_k$  as the desired signal and the other terms of (17) as worst-case Gaussian noise when decoding the signal. Consequently, a lower bound for the ergodic achievable SE at the kth user can be written as [16]

$$S_{k} = \mathbb{E}\left[\log_{2}\left(1 + \frac{p_{k} \left|\mathbf{w}_{k}^{H}\mathbf{g}_{k}\right|^{2}}{\sum_{i \neq k} p_{i} |\mathbf{w}_{k}^{H}\mathbf{g}_{i}|^{2} + \left|\mathbf{w}_{k}^{H}\mathbf{n}\right|^{2} + \left|\mathbf{w}_{k}^{H}\mathbf{U}^{-1}\mathbf{q}\right|^{2}}\right)\right].$$
(18)

## IV. NUMERICAL RESULTS

In this section, we numerically evaluate the SE performance of the  $\Sigma\Delta$  massive MIMO system for various scenarios. We assume static-aware power control in the network [17] so that  $p_k = p_0/\beta_k$ . In all of the cases considered, unless otherwise noted, we assume K = 10 users and equally spaced antennas with normalized spacing d. The DoAs for each user are drawn uniformly from the interval  $[\theta_0 - \delta, \theta_0 + \delta]$ , and the center angle of the  $\Sigma\Delta$  array is steered towards  $\phi = 2\pi d\sin(\theta_0)$ .

To highlight the impact of mutual coupling, we will compare the performance when mutual coupling is included to that

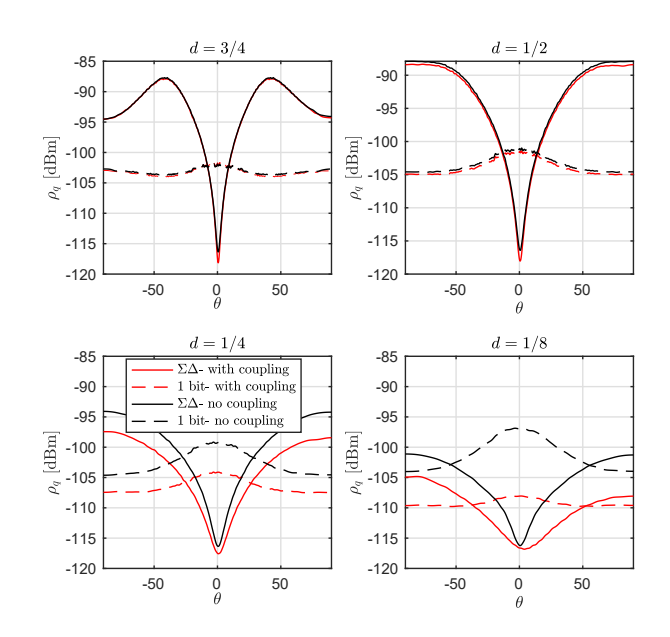


Fig. 1. Quantization noise power density for a system with  $\theta_0 = 0^\circ$ ,  $2\delta = 40^\circ$ , SNR = 0 dB, M = 100, L = 15.

when it is hypothetically absent. Simulating the case without mutual coupling amounts to setting Z = RI in (3) and (6), which leads to  $T = \frac{1}{2}I$  and  $R_n = \sigma_n^2 I$ , with the noise power

$$\sigma_n^2 = \frac{1}{4} \left[ \sigma_i^2 \left( R^2 + R_N^2 - 2R_N R \Re(\rho) \right) + 4kTBR \right].$$

The factor of 1/2 in T results from the fact that x in (1) is the voltage on a load matched to the antenna impedance. This voltage is half of the antenna open-circuit voltage, and given that the load represents the input to the LNA, it is the signal available for further processing. Thus, the per-antenna and peruser reference signal-to-noise-ratio (SNR) in the absence of mutual coupling is given by

$$SNR \triangleq \frac{1}{4} \frac{p_0}{\sigma_n^2}.$$
 (19)

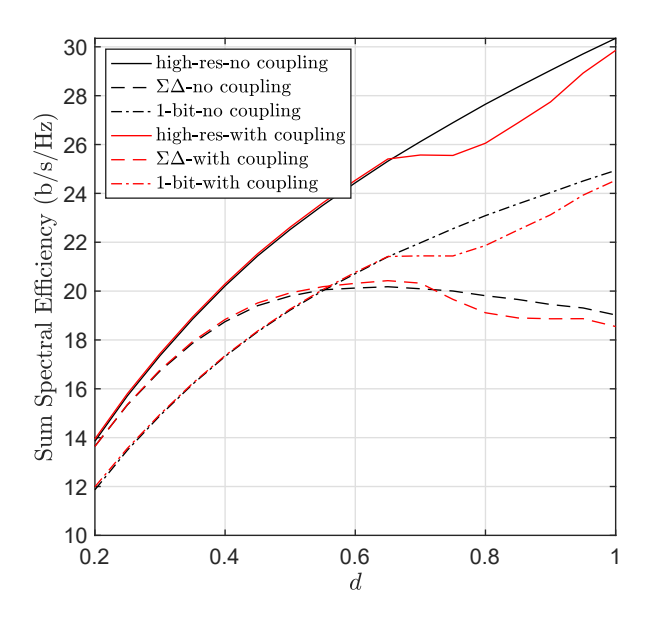
The circuit parameters used in (3) and (6) are defined as  $\sigma_i^2$  = 2kTB/R, and  $\sigma_u^2 = 2kTBR$ , leading to  $R_N = R$  where R = R50  $\Omega$ , T=290 K,  $\rho=0$ , and B=20 MHz. This leads to a value of  $\sigma_n^2 = 2kTBR$ , where the factor of 2 appears because we are accounting for noise in both the antennas and the LNAs. We further assume CSCG symbols and 10<sup>4</sup> Monte Carlo trials for the simulations.

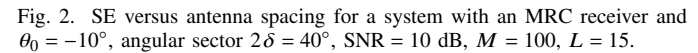
In Fig. 1, we investigate the impact of the mutual coupling matrix, T, on the spatial spectrum of the quantization noise when  $\theta_0 = 0$ . To do so, we define the quantization noise power density as

$$\rho_{q}(\theta) \triangleq \frac{1}{c(\theta)} \mathbb{E}\left[\left|\boldsymbol{a}(\theta)^{H} \boldsymbol{T}^{H} \boldsymbol{U}^{-1} \boldsymbol{q}\right|^{2}\right], \tag{20}$$

where  $c(\theta) = \|Ta(\theta)\|^2$  is a normalizing factor and  $\theta \in$  $[-90^{\circ}, 90^{\circ}]$  denotes the DoA. We see that the noise shaping

110





100 Sum Spectral Efficiency (b/s/Hz) 90 high-res-no coupling  $\Sigma\Delta\text{-no coupling}$ 80 1-bit-no coupling high-res-with coupling 70  $\Sigma\Delta$ -with coupling 1-bit-with coupling 60 50 40 30 20 0.2 0.4 0.6 8.0 1

Fig. 3. SE versus antenna spacing for a system with ZF receiver and  $\theta_0 = -10^{\circ}$ , angular sector  $2\delta = 40^{\circ}$ , SNR = 10 dB, M = 100, L = 15.

characteristic of the  $\Sigma\Delta$  array is not significantly affected by the mutual coupling, except for the case of  $d = \lambda/8$ , where we see a small shift in the quantization noise spectrum.

In Fig. 2, we show the effect of antenna spacing on the SE of a system with an MRC receiver. We see that, when there is no constraint on the size of the array, better performance for the standard one-bit architecture can be achieved by moving the antennas farther apart. We see that the standard one-bit architecture outperforms the  $\Sigma\Delta$  array when  $d>\lambda/2$ , due to the fact that increasing the antenna spacing increases the quantization noise power for the  $\Sigma\Delta$  architecture across the DoA sector of interest, as observed in Fig. 1. Furthermore, we see that the SE for the  $\Sigma\Delta$  architecture is not monotonic and  $d=\lambda/2$  provides the best performance, which corresponds to no oversampling. The optimal value of d for the  $\Sigma\Delta$  array will of course decrease if the sector of user DoAs was widened.

The SE results for the ZF receiver are shown in Fig. 3. We again observe the degradation of the  $\Sigma\Delta$  performance as d increases, but in this case there is a more significant gain relative to standard one-bit quantization for smaller antenna spacings, and the optimal antenna spacing for the  $\Sigma\Delta$  array is reduced to approximately  $d = \lambda/3$ .

While the standard one-bit architecture can outperform the  $\Sigma\Delta$  approach when there is no constraint on the dimension of the array (large d), Figs. 4 and 5 demonstrate that the  $\Sigma\Delta$  array provides a better result in space-constrained scenarios. For these simulations, we consider a case in which the antenna array has a limited aperture of  $d_0 = 50$  and we increase the number of antennas from M = 100 to M = 400, which corresponds to a decrease in antenna spacing from d = 1/2 to d = 1/8. For the case of an MRC receiver in Fig. 4, the  $\Sigma\Delta$  architecture achieves a spectral efficiency nearly equal to that

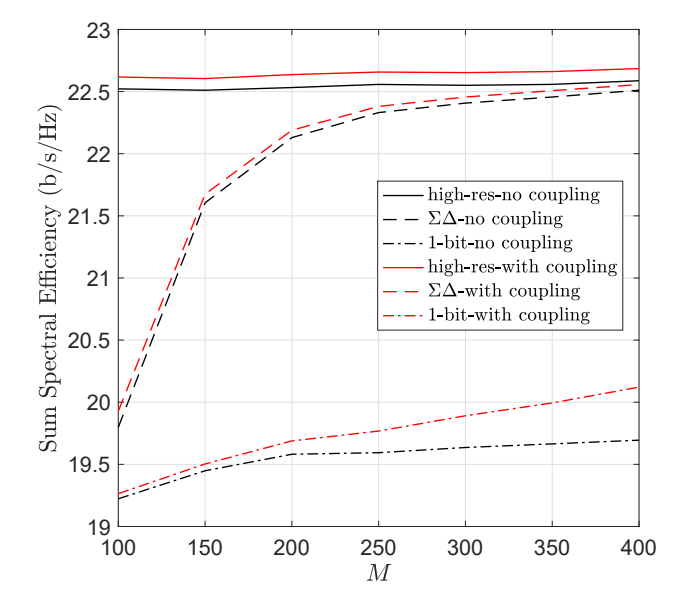
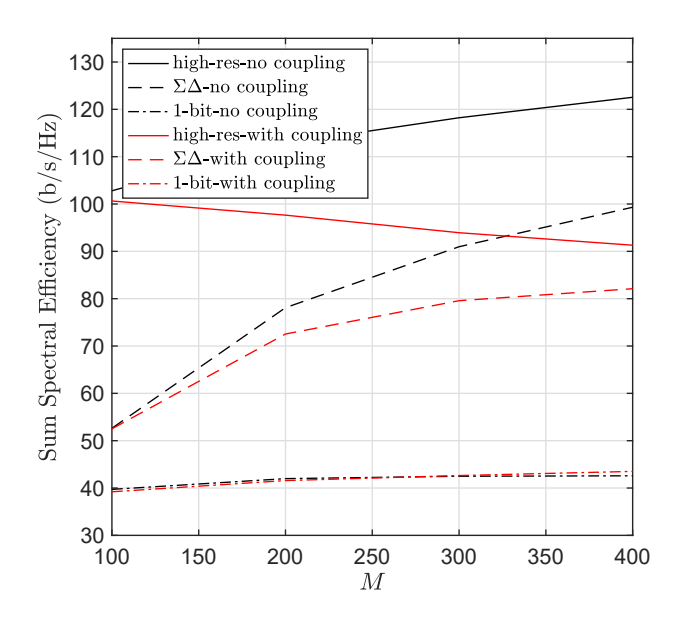
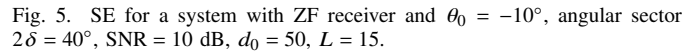


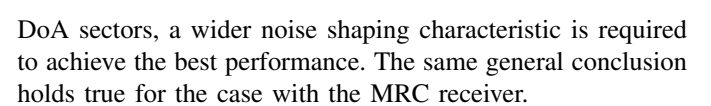
Fig. 4. SE versus number of BS antennas for a system with MRC receiver and  $\theta_0 = -10^\circ$ , angular sector  $2\delta = 40^\circ$ , SNR = 10 dB,  $d_0 = 50$ , L = 15.

of an array with full-resolution ADCs when  $M \ge 250$ . For the case of ZF,  $\Sigma\Delta$  provides a dramatic gain in SE over standard one-bit quantization.

In Fig. 6, the optimal antenna spacing for the  $\Sigma\Delta$  architecture with a ZF receiver is shown for different SNRs, where we have quantized d to the nearest value of  $\lambda/10$ . It can be seen that the optimal spacing is dependent on the SNR and DoA region width,  $\delta$ . The optimal antenna spacing decreases as SNR increases, and also as the size of the DoA sector of interest increases. We expect this phenomenon since for wider







#### V. Conclusion

We have studied the effect of mutual coupling on the performance of one-bit  $\Sigma\Delta$  massive MIMO systems. It was shown that the  $\Sigma\Delta$  architecture is most suitable for array deployments with an aperture size constraint. While the performance of standard one-bit quantization saturates as the number of antennas increases in a constrained-aperture array, the performance of the  $\Sigma\Delta$  architecture tends to approach that of a system with high-resolution ADCs. This is due to the noise-shaping gain achieved by the  $\Sigma\Delta$  architecture when the users are sectorized or the array is oversampled in space. It is worthwhile to note that the inevitable power loss due to mutual coupling can to some extent be alleviated using, for example, a matching network. This is a subject of future investigation.

# REFERENCES

- L. Fan, S. Jin, C. Wen, and V. Zhang, "Uplink achievable rate for massive MIMO systems with low-resolution ADC," *IEEE Commun. Lett.*, vol. 19, no. 12, pp. 2186-2189, Dec. 2015.
- [2] C. Mollén, J. Choi, E. G. Larsson, and R. W. Heath, "Uplink performance of wideband massive MIMO with one-bit ADCs," *IEEE Trans. Wireless Commun.*, vol. 16, no. 1, pp. 87–100, Jan 2017.
- [3] J. Zhang, L. Dai, S. Sun, and Z. Wang, "On the spectral efficiency of massive MIMO systems with low-resolution ADCs," *IEEE Commun. Lett.*, vol. 20, no. 5, pp. 842-845, May. 2016.
- [4] Y. Li, C. Tao, L. Liu, A. Mezghani, G. Seco-Granados, and A. Swindle-hurst, "Channel estimation and performance analysis of one-bit massive MIMO systems," *IEEE Trans. Signal Process.*, vol. 65, no. 15, pp. 4075-4089, May 2017.
- [5] S. Jacobsson, G. Durisi, M. Coldrey, U. Gustavsson, and C. Studer, "Throughput analysis of massive MIMO uplink with low-resolution ADCs," *IEEE Trans. Wireless Commun.*, vol. 16, no. 6, pp. 4038–4051, June 2017.

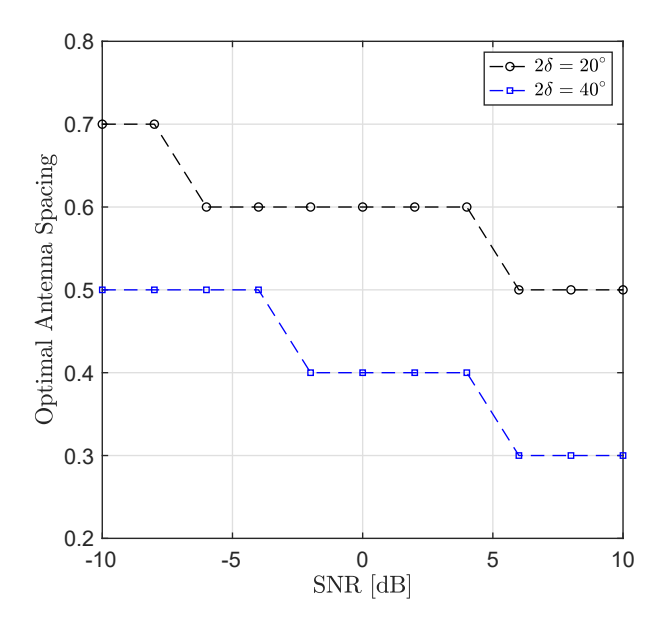


Fig. 6. Optimal antenna spacing versus SNR for a system with ZF receiver and  $\theta_0 = -10^{\circ}$ , M = 100, L = 15.

- [6] Y. Li, C. Tao, A. L. Swindlehurst, A. Mezghani, and L. Liu, "Downlink achievable rate analysis in massive MIMO systems with one-bit DACs," *IEEE Commun. Lett.*, vol. 21, no. 7, pp. 1669–1672, July 2017.
- [7] D. Barac and E. Lindqvist, "Spatial sigma-delta modulation in a massive MIMO cellular system," Master's thesis, Department of Computer Science and Engineering, Chalmers University of Technology, 2016.
- [8] H. Pirzadeh, G. Seco-Granados, S. Rao, and A. Swindlehurst, "Spectral efficiency of one-bit Sigma-Delta massive MIMO," arXiv.org Oct. 2019. Available: http://arxiv.org/abs/1910.05491.
- [9] M. Shao, W. Ma, Q. Li and A. L. Swindlehurst, "One-Bit Sigma-Delta MIMO Precoding," *IEEE J. Sel. Topics Signal Process.*, vol. 13, no. 5, pp. 1046-1061, Sep. 2019.
- [10] S. Rao, H. Pirzadeh and A. Swindlehurst, "Massive MIMO channel estimation with 1-bit spatial Sigma-Delta ADCs," in *Proc. IEEE Int. Conf. Acous., Speech, Signal Process. (ICASSP)*, May 2019, pp. 4484–4488.
- [11] C. Masorous, M. Sellathurai, and T. Ratnarajah, "Large-Scale MIMO transmitters in fixed physical spaces: The effect of transmit correlation and mutual coupling," *IEEE Trans. Commun.*, vol. 61, no. 7, pp. 2794-2804, July 2013.
- [12] S. Biswas, C. Masorous, and T. Ratnarajah, "Performance analysis of large multiuser MIMO systems with space-constrained 2-D antenna arrays," *IEEE Trans. Wireless Commun.*, vol. 15, no. 5, pp. 3492-3505, May 2016.
- [13] S. A. Schelkunoff, Antennas: Theory and Practice. New York: John Wiley and Sons, 1952.
- [14] M. T. Ivrlac and J. A. Nossek, "Toward a circuit theory of communication," *IEEE Trans. Circuits Syst. I, Reg. Papers*, vol. 57, no. 7, pp. 1663–1683, July 2010.
- [15] H. Q. Ngo, E. G. Larsson, and T. L. Marzetta, "The multicell multiuser MIMO uplink with very large antenna arrays and a finite-dimensional channel," *IEEE Trans. Commun.*, vol. 61, no. 6, pp. 2350-2361, June 2013.
- [16] Q. Zhang, S. Jin, K-K. Wang, H. Zhu, and M. Matthaiou "Power scaling of uplink massive MIMO systems with arbitrary-rank channel means," *IEEE Journal of Sel. Topics Sig. Process.*, vol. 8, no. 5, pp. 966-981, Oct. 2014.
- [17] E. Björnson, E. G. Larsson, and M. Debbah, "Massive MIMO for maximal spectral efficiency: How many users and pilots should be allocated?," *IEEE Trans. Wireless Commun.*, vol. 15, no. 2, pp. 1293-1308, Feb. 2016.